

Primljen / Received: 3.8.2023.

Ispravljen / Corrected: 6.12.2023.

Prihvaćen / Accepted: 7.12.2023.

Dostupno online / Available online: 10.2.2024.

Failure analysis of hybrid strengthened RC square column

Authors:

Assist.Prof. **Vivekanandan R**, M.E.Government College of Engineering, Sengipatti
Department of Civil Engineering
Thanjavur, Indiarvivekanandan@gcetj.edu.in

Corresponding author

Assoc.Prof. **Aarthi Karmegam**, PhD. CEGovernment College of Engineering, Bodinayakanur
Department of Civil Engineering
Indiaaarthi_karmegam@yahoo.co.in

Research Paper

Vivekanandan R, Aarthi Karmegam

Failure analysis of hybrid strengthened RC square column

This paper presents an analytical and experimental examination of reinforced concrete (RC) columns strengthened with a combined system of fibre-reinforced cementitious material (FRCM) and externally bonded fibre-reinforced plastics (EB-FRP). The proposed technique makes use of these advantages in enhancing the strength and minimising the premature failure of RC columns. Seven square RC columns were cast: one control column, four FRCM-strengthened columns, and two hybrid-strengthened columns. Two fibres, namely, carbon and glass fibres, were used. The columns were tested under an axial compression load in a loading frame. The ultimate strength, load vs. deformation, failure, and ductility were discussed to examine the failure and strengthening behaviour. The proposed method provided a higher confinement effect and increased capacity with fewer FRCM with EB-FRP than the other methods. Analytical predictions of the peak load were made and correlated with the experimental results.

Key words:

FRP, FRCM, hybrid, RC column, wrapping, confinement, carbon FRP (CFRP), glass FRP (GFRP)

Prethodno priopćenje

Vivekanandan R, Aarthi Karmegam

Analiza sloma hibridno ojačanog AB kvadratnog stupa

Ovaj rad predstavlja analitičko i eksperimentalno ispitivanje armiranobetonskih (AB) stupova ojačanih kombiniranim sustavom cementnog materijala ojačanog vlaknima (engl. *fibre-reinforced cementitious material* - FRCM) i vanjski povezan vlaknima ojačan polimer (engl. *externally bonded fibre-reinforced plastics* - EB-FRP). Predložena tehnika iskorištava ove prednosti za povećanje čvrstoće i smanjenje preranog sloma AB stupova. Izliveno je sedam kvadratnih AB stupova: jedan obični stup, četiri stupa ojačana FRCM-om i dva hibridno ojačana stupa. Upotrijebljene su dvije vrste vlakana: ugljična i staklena vlakna. Stupovi su ispitani pod aksijalnim tlačnim opterećenjem u okviru za opterećenje. Razmatrana je granična čvrstoća, opterećenje u odnosu na deformaciju, slom i duktilnost kako bi se ispitala faza očvršćivanja i sloma. Predložena metoda omogućila je veći utjecaj ovijenosti i povećani kapacitet s manjim brojem FRCM-a s EB-FRP-om u odnosu na ostale metode. Napravljena su analitička predviđanja vršnog opterećenja te su korelirana s eksperimentalnim rezultatima.

Ključne riječi:

vlaknima ojačani polimer (FRP), vlaknima ojačani cementni materijal (FRCM), hibrid, AB stup, omatanje, ovijenost, ugljičnim vlaknima ojačani polimer (CFRP), staklenim vlaknima ojačani polimer (GFRP)

1. Introduction

Most buildings worldwide are constructed using reinforced concrete. The major causes of the damages in the existing reinforced concrete structures are design deficiencies, strength inadequacy, natural calamities, errors in construction, durability, accidental loads, etc [1-6]. Different strengthening methods are available to minimise the effect of damages and extend the life of structures. In developing fibre-reinforced plastics (FRP) materials, different FRP techniques have been developed and used because of their distinct properties, such as high tensile capacity, high strength-to-weight ratio, and easy handling; however, FRP also has some disadvantages, such as inappropriate use in fire environments, wet surfaces, and inadequate bonding with concrete surfaces. Additional treatment is required to counter these environments [7-11].

Various FRP techniques, such as external jacketing of FRP bars, externally bonded FRP (EB-FRP), near surface mounted (NSM) method, and fibre-reinforced cementitious material (FRCM) methods, make it possible to strengthen weakened elements in RC buildings [15-25]. Strengthening using FRP bars involves the use of composite materials to enhance the structural performance of concrete elements such as beams or columns. FRP bars are composed of high-strength fibres, such as carbon or glass, embedded in a polymer resin matrix. This method is an alternative to traditional steel reinforcement, and is often used to retrofit or upgrade existing structures. Externally bonded FRP is a method of reinforcing structures, particularly concrete structures, using FRP materials on the external surface. FRP composites are composed of fibres such as carbon fibres, glass fibres, or aramid fibres embedded in a resin matrix. In externally bonded FRP, composite materials are applied to the exterior surface of a structure to enhance its strength, durability, and load-bearing capacity. The near surface-mounted (NSM) FRP method has been used in structural engineering to strengthen and reinforce concrete structures. In this method, FRP materials, which typically consist of fibres, such as carbon or glass, embedded in a resin matrix, are applied within grooves or slots cut into the near-surface region of a concrete element. Among the different techniques, the FRCM technique has been used in recent years and provides better performance in retrofitting RC elements by providing a higher capacity and stiffness to damaged RC elements [26-28]. Comparing the different fibres, the Carbon FRCM resulted in a higher strength [12, 29]. Noor Tello et al. examined the behaviour of a polyparaphenylene benzo-bisoxazole fibre reinforced cementitious material (PBO-FRCM) strengthened column, and their results indicated higher strength and ductility [30]. The circular column exhibited better confinement than the square column owing to the corner effect. The FRCM method provided good results for the retrofitting of RC elements to obtain sufficient ultimate capacity, ductility, and stiffness. Although the FRCM method exhibits good results in strengthening/retrofitting, the effect on the ultimate capacity and ductility decreases when the number of FRCM layers increases [16-19, 31-36]. The failure of the FRCM is caused by the slippage of the fibre inside the

cementitious matrices rather than by fibre rupture. The thickness of the column increases when the number of FRCM layers increases, leading to floor space constraints [8, 19, 34]. More than two FRCM layers were ineffective because of the easy deposition of FRCM layers off the concrete substrate.

To mitigate the strengths and weaknesses inherent in individual techniques, one strategy involves combining two or more methods to improve the overall performance of the column behaviour, referred to as hybridisation. The combination of two methods/techniques in the strengthening of reinforced concrete elements exhibits better behaviour, such as ultimate capacity, failure pattern, and shear behaviour. The hybridisation of different methods helps to enhance the capacity, stiffness, confinement, and ductility, and alters the mode of failure owing to the advantages of one method over another [1, 2, 39, 40]. Chellapandian et al. investigated RC columns strengthened with hybrid near surface mounted/externally bonded FRP (NSM/EB-FRP) under eccentric compression and concluded that the method yields higher ultimate strength and ductility of 51 % and 272 %, respectively [15, 37]. Amit Saini and Surya Prakash studied hybrid EB/NSM FRP strengthened slender columns and demonstrated an increased ductility of more than 30 % [1]. Medinelspir et al. investigated hybrid CFRP and GFRP in terms of the effectiveness of confinement on RC columns and showed higher confinement and ductility [40]. Wakjira et al. experimentally investigated an RC column with a hybrid NSM/EB-FRCM and demonstrated a higher shear capacity, ultimate capacity, and deformation characteristics [38].

Previous studies on the strengthening of RC elements using hybrid techniques have been limited. The hybrid method helps to improve the performance of RC elements in terms of shear, flexure, and compression. However, the use of the hybrid method is limited because of the lack of experimental evidence. In the present study, experiments were conducted on an RC square column to analyse the effectiveness of the hybrid FRCM/EB-FRP over the FRCM method only. Further, two types of fibres (carbon and glass) were used. The strengthening configurations of single-layer FRCM, double-layer FRCM, and hybrid FRCM/EB-FRP were used to verify the effectiveness of the hybrid method. This study reveals the effectiveness of the hybrid method over FRCM only in terms of the ultimate capacity, deformation characteristics, ductility, and mode of failure. This novel hybrid method is expected to overcome the disadvantages of FRCM, maximise the strengthened column capacity, and minimise the thickness of the strengthened column.

2. Analytical model

An analytical model was used to predict the behaviour of the RC column using a strain compatibility procedure. The load–displacement curve was constructed using fibre section analysis. This analysis is known as the layer-by-layer approach. In this analysis, the cross section of the element is subdivided into a number of layers of smaller thickness “ t ” (Figure 1). The model provided estimated stress values.

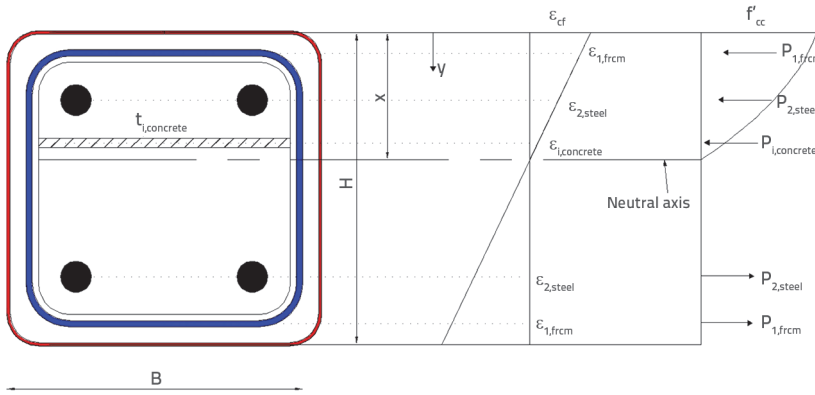


Figure 1. Method of discretization of the RC column element using the fiber element approach: a) Cross section of the column; b) strain profile; c) Force and stress diagram

$$f_c = 2f'_c \left[\frac{\frac{\epsilon_c}{\epsilon'_c}}{1 + \left(\frac{\epsilon_c}{\epsilon'_c}\right)^2} \right] \quad 0,002 < \epsilon_c < 0,0035 \quad (2)$$

2.2. Confined concrete model

Mander et al. developed the confinement model by considering factors such as ultimate confined strain (ϵ_{cc}), elastic modulus E_c , and confined compression stress (f'_{cc}) in the normalised stress-strain equation of Popovics [47, 48]. Subsequently, Lam and Teng developed a design-oriented model for confined concrete with EB-FRP (Figure 2) [45, 46]. The Mander et al. model is valid only for steel confinement and overestimates the FRP confinement strength. The confined concrete stress (f_c) was calculated using Equation (5) and the values of the corresponding parameters such as slope of linear portion (E_2) and transition strain (ϵ'_t) can be estimated using Equations (4) and (5).

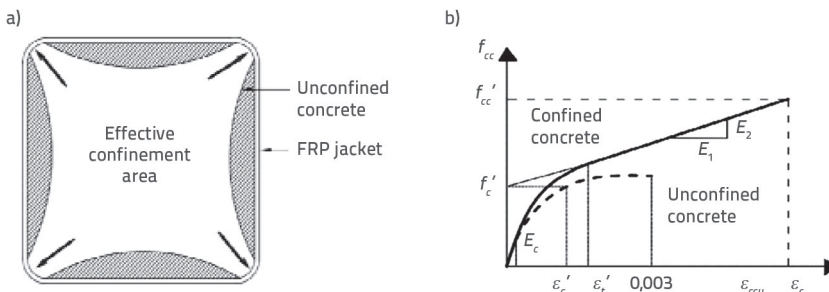


Figure 2. Lam and Teng model and the effect of square confinement: a) Confinement effect in square section; b) Lam and Teng model

The modified Hognestad's Equations (1) and (2) were used to calculate the stress value in each layer. In the model analysis, Hognestad's analytical model was used for analytical predictions of unconfined concrete and the Lam and Teng model was used for confined concrete [43-46]. A constitutive relationship was used to obtain the stress-strain relationship between the steel and the FRPs..

2.1. Un-Confined concrete model

Hognestad's parabolic model was used to predict the stress in unconfined concrete elements (f_c) under compression [44]. The total load (P_c) contribution can be calculated using Equations (1) and (2). Equations (1) and (2) predict the pre-peak and post-peak behaviours of the concrete stress-strain behaviour. Equation (2) is a modified equation for the post-peak behaviour of concrete proposed by Hognestad. The modified equation yields analytically predicted results that are close to the experimental results. The contribution of the force by the steel bars P_s was calculated using its stress - strain relationship, and the total force P_t was determined. The peak strain (and ultimate strain (were assumed to be 0.002 and 0.0035, respectively.

$$f_c = f'_c \left[2 \frac{\epsilon_c}{\epsilon'_c} - \left(\frac{\epsilon_c}{\epsilon'_c} \right)^2 \right] \quad 0 < \epsilon_c < 0,002 \quad (1)$$

$$f_c = \begin{cases} E_c \epsilon_c - \frac{(E_c - E_2)^2}{4f'_c} \epsilon_c^2 & 0 < \epsilon_c < \epsilon'_t \\ f'_c + E_2 \epsilon_c & \epsilon'_t \leq \epsilon_c \leq \epsilon_{ccu} \end{cases} \quad (3)$$

$$E_2 = \frac{f'_{cc} - f'_c}{\epsilon_{ccu}} \quad (4)$$

$$\epsilon'_t = \frac{2f'_c}{E_c - E_2} \quad (5)$$

$$f'_{cc} = f'_c \left(1 + \psi_f \cdot 3.3 k_a \frac{f_l}{f'_c} \right) \quad (6)$$

$$f_l = \frac{2E_t n t_f \epsilon_{fe}}{D} \quad i \epsilon_{fe} = k_\epsilon \cdot \epsilon_{fu} \quad (7)$$

$$k_a = \frac{A_g}{A_c} \left(\frac{b}{h} \right)^2 \quad i \quad k_b = \frac{A_g}{A_c} \left(\frac{b}{h} \right)^{0.5} \quad (8)$$

$$\frac{A_g}{A_c} = \frac{1 - \left[\left(\frac{b}{h} \right) \left((h - 2r_c) \right)^2 \left(\frac{h}{b} \right) \left((b - 2r_c) \right)^2 \right]}{3A_g - 1 - \rho_g} \quad (9)$$

The maximum confined compressive strength of the concrete (f_{cc}) was calculated in terms of the maximum confinement pressure (f_l), as described in Equations (10) and (11). The value of the additional reduction factor Ψ_f was taken as 0.95. The shape factors (k_o and k_d) used for the noncircular columns were calculated using Equation (8). For the circular column, the shape factors were set to 1. The A_e/A_c ratio was calculated using Equation (9). The most important parameter of the confined model was the corner radius (r_c) which was taken as 10 mm.

3. Experimental setup

The Experiment consisted of seven RC columns with dimensions of 150 mm × 150 mm, and a total height of 600 mm. The columns were cast and cured for four weeks. Before pouring the concrete, strain gauges were fixed at both the middle and end ties, as shown in Figure 8. After sufficient curing, the FRCM layer was laid over the column specimen and rested for two days to obtain sufficient bonding strength. Before applying the epoxy coating, the surface was cleaned to remove dirt, debris, and any unwanted particles using a compressed air-brushing machine. For the hybrid specimen, an epoxy coating (2 mm) was applied over the FRCM layer, and a small amount of sand was blasted on the bonded surface to achieve good bonding with the FRP. The FRP was wrapped over an epoxy-coated specimen.

Figure 3 shows a schematic of the loading setup. A representation of the column designation ID is shown in Figure 4, and Table 1 explains each specimen. The seven cast columns are shown in Figure 5. The loading frame setup and LVDT arrangements are shown in Figure 6. The columns were tested at the loading rate of 1 kN/s. A loading cell was placed on top of the specimen and connected to a Data Acquisition system (DAQ).

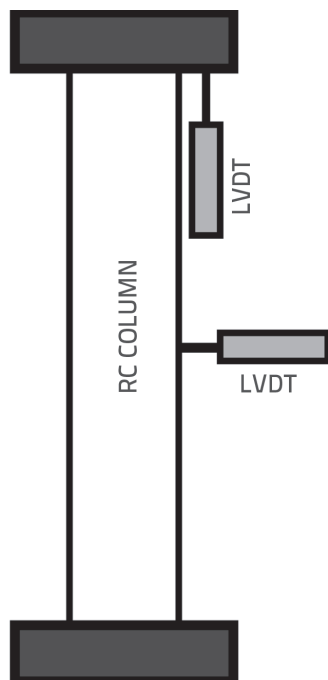


Figure 3. Schematic instrument setup

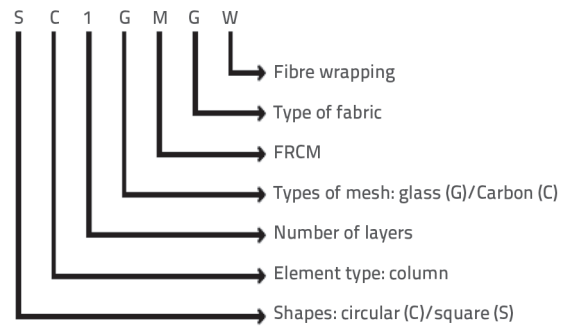


Figure 4. Square column designation ID



Figure 5. Seven square columns



Figure 6. Experimental setup - loading frame and LVDT arrangements: a) Loading frame; b) LVDT

3.1. Materials

The seven columns were cast in three batches. According to IS 456-2000, a nominal mix of M20 grade concrete and mix and Fe500 grade steel were used. One cubic meter of concrete consisted of 360 kg of cement, 585 kg of fine aggregates, and 1223 kg of coarse aggregates, and a w/c ratio of 0.5. OPC 53 Grade cement and a maximum aggregate size of 10 mm were used. For each batch of concrete, three cubes and three cylinders were fabricated to ensure the compressive and tensile strengths of the concrete as per IS 456-2000, and the sample results are provided in Table 2. The longitudinal reinforcement consisted of four 10 mm diameters, and the transverse reinforcement consisted of three

Table 1. Specimen designation and its descriptions

Specimen ID	Description
SCC	Square control column
SC1GM	RC square column strengthened with single layer glass FRCM
SC2GM	RC square column strengthened with double layer glass FRCM
SC1GMGW	RC square column strengthened with single layer glass FRCM and external epoxy bonded glass FRP wrapping
SC1CM	RC square column strengthened with single layer carbon FRCM
SC2CM	RC square column strengthened with double layer carbon FRCM
SC1CMCW	RC square column strengthened with single layer carbon FRCM and external epoxy bonded carbon FRP wrapping

Table 2. Concrete properties

Sl. No.	Stages	Specimen	Compression strength [N/mm ²]	Average compression strength [N/mm ²]	Cube or cylinder	Splitting tensile strength [N/mm ²]	Average split tensile strength [N/mm ²]
1	I	Cube 1	22.81	23.35	Cylinder 1	2.10	2.22
2		Cube 2	24.59		Cylinder 2	2.31	
3		Cube 3	21.26		Cylinder 3	2.35	
4	II	Cube 1	23.11		Cylinder 1	2.33	
5		Cube 2	23.50		Cylinder 2	2.41	
6		Cube 3	25.56		Cylinder 3	2.39	
7	III	Cube 1	23.33		Cylinder 1	2.09	
8		Cube 2	23.20		Cylinder 2	2.03	
9		Cube 3	22.82		Cylinder 3	2.00	

6 mm diameters spaced at 250 mm C/C. The longitudinal bars were bent to 90o at the end to address bearing. The details of the reinforcement are shown in Figure 7. The fixation of the strain gauge is shown in Figure 8. Images of the glass and carbon fabrics and mesh are shown in Figure 9. The properties of the strain gauge, fibre fabric, and Fibre Mesh are listed in Table 3, Table 4, and Table 5. The sequential procedure of strengthening using FRCM and External FRP bonding are shown in Figure 10.

Table 3. Strain gage properties

Gauge length	Resistance	Gauge factor
5mm	350 ± 0.5 ohms	1.9

Table 4. Properties of fabric

Type of fibre	Glass	Carbon
Elongation	0.048	0.017
Area weight	200 g/m ²	230 g/m ²
Tensile strength	3400 MPa	4130 MPa
Sheet thickness	0.255 mm	0.255 mm

Table 5. Properties of fibre mesh

Type of fibre	Glass	Carbon
Elongation	4.70 %	1.70 %
Area weight	145 g/m ²	230 g/m ²
Size of mesh	5 mm × 5 mm	10 mm × 10 mm
Sheet thickness	0.175 mm	0.255 mm

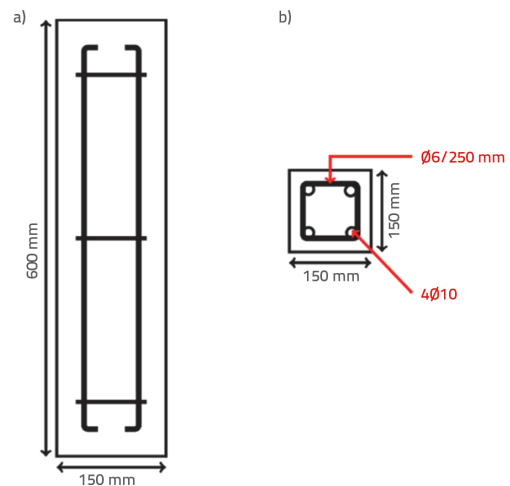


Figure 7. Reinforcement detailing RC circular column: a) Longitudinal section; b) Cross section



Figure 8. Strain gage fixation

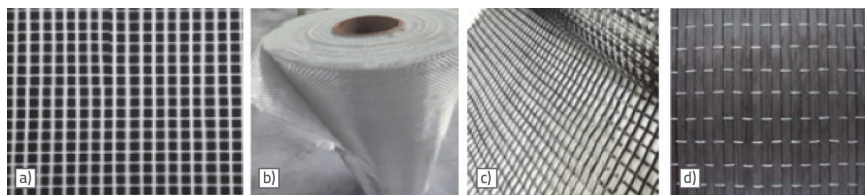


Figure 9. Fibre mesh and Fabric a) GFRP mesh; b) GFRP fabric; c) CFRP mesh; d) CFRP fabric

experimental results and analytical predictions.

4.1. Ultimate strength

The test results of the ultimate load and deformation in the three directions for all specimens, namely SCC, SC1GM, SC2GM, SC1GMGW, SC1CM, SC2CM, and SC1GMCW, are listed in Table 6. The percentage increase in the ultimate strength of the strengthened specimens compared to that of the control specimen is shown in Figure 11. As shown in Figure 11, all the strengthened specimens exhibited a higher ultimate strength at failure than the control specimen. The columns with single- and double-layer glass/carbon FRCM, such as SC1GM, SC2GM, SC1CM, and SC2CM, exhibited capacities of 10 % to 30 % higher than that of the control specimen. The hybrid-strengthened specimens SC1GMGW and SC1GMCW exhibited improved performance, yielding a peak strength increase of 25 % to 50 % under axial compression compared with reference specimen. When compared with the FRCM-strengthened specimen, the proposed hybrid method demonstrated 15 % to 25 % higher peak load capacity. This indicates that the hybrid strengthening techniques effectively enhanced the column behaviour by providing a higher confining action and that the combined FRCM/EB-FRP system exhibited a superior peak capacity compared to its counterparts. In the hybrid method, the external fibres absorb excessive loading on the column and yield, ensuring the safety of the column against failure. When comparing the hybrid-strengthened specimen to a column strengthened solely with FRCM, the hybrid FRCM/EB-FRP approach attained a greater strength with fewer FRCM layers, consequently reducing the thickness of the strengthening layer around the column. The corners of the square column were rounded to a 10 mm radius, which improved the bonding between the fibre and concrete surface and helped minimise the edge effect. Figure 12 shows a comparison of the experimental load with the analytical predictions. The analytical predictions slightly overestimated the peak load compared to the experimental load.



Figure 10. Strengthening sequences of RC square column a) Glass FRCM/FRP wrapping and b) Carbon FRCM/FRP wrapping

4. Results and discussion

All the seven columns were tested under axial compression in the loading frame at a loading rate of 1kN/s. In this section, the ultimate capacity, load versus vertical deformation, ductility, and failure patterns are discussed and compared with the

Table 6. Test results

No.	Specimen ID	Percentage of reinforcement ρ_s	Granična nosivost P_{max} [kN]	Deformation Δy (axial) at ultimate load [mm]	Deformation Δx (lateral) at ultimate load [mm]	Deformation Δz (lateral) at ultimate load [mm]	Failure pattern
1	SCC	0.014	241.0	9.6	0.9	3.6	Crushing failure
2	SC1GM	0.014	268.7	9.3	0.7	7.4	Mortar crushed, fibre rupture
3	SC2GM	0.014	284.8	6.3	2.5	5.5	Mortar delamination, fibre slippage and rupture
4	SC1GMGW	0.014	310.6	6.8	3.5	2.9	Fibre yielding/tearing
5	SC1CM	0.014	302.4	5.9	0.9	1	Mortar delamination, fibre rupture
6	SC2CM	0.014	314.8	5.7	3.2	2.7	Mortar delamination, fibre slippage and rupture
7	SC1GMCW	0.014	369.0	4.8	3.3	3.3	Fibre de-bonded and wrinkled

The test results of the ultimate load and deformation in the three directions for all specimens, namely SCC, SC1GM, SC2GM, SC1GMGW, SC1CM, SC2CM, and SC1GMCW, are listed in Table 6. The percentage increase in the ultimate strength of the strengthened specimens compared to that of the control specimen is shown in Figure 11.

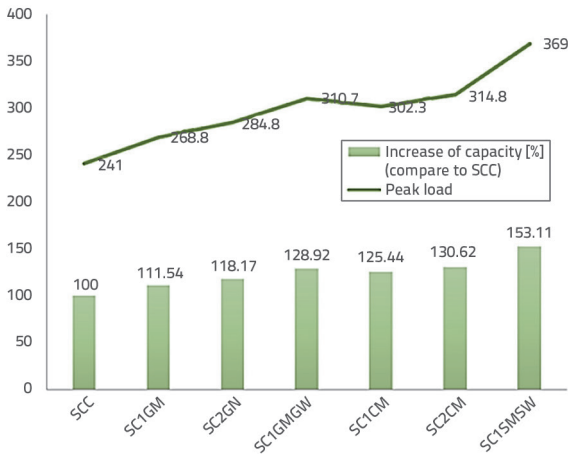


Figure 11. Percentage increment of ultimate compared with control specimen (considered control column capacity taken as 100 %)

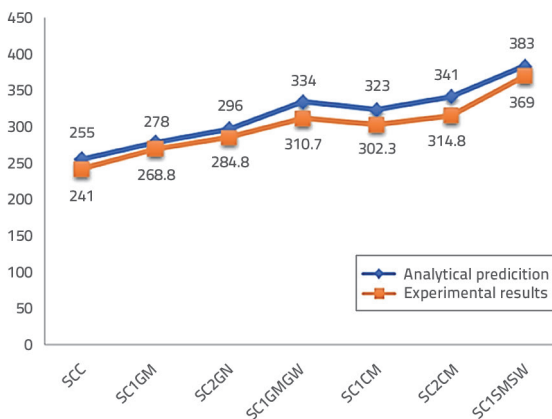


Figure 12. Experimental load vs. analytical prediction

4.2. Load vs. deformation

The Load vs. deformation curve helps understand the behaviour of the RC elements, and the corresponding load vs. axial deformation curves for all specimens are shown in Figures 13 and 14. The behaviours of all strengthened specimens showed similar responses irrespective of the fibre type. When the strengthened columns were loaded, the columns exhibited linear behaviour up to 75 % to 85 % of the peak load, showing elastic behaviour. At the beginning of the load–deformation curves at lower strains, the control and strengthened specimens exhibited similar responses. This similarity occurred because the compression loads were primarily absorbed by the concrete core, and the strengthening layers were not yet influenced. As the load approached the peak value, the strengthened columns diverged from those of the

unconfined column, and the external FRCM/FRP layers developed a confining action. The enhanced specimens exhibited lower yield and peak displacements than the control specimens, which was attributed to improvements in the initial stiffness of the specimen, as shown in Figures 13 and 14. Fibre yielding progressed around the peak load and a higher deformation was observed. Ultimately, the columns failed due to concrete crushing, which was possibly because of the use of lower-grade concrete. The hybrid FRP-strengthened specimens exhibited superior performance in enhancing overall behaviour, resulting in a notable increase in strength by approximately 50 % respectively. Furthermore, the onset of FRP splitting cracks on the tension side at 80 % of the peak load highlighted the crucial role of lateral confinement in delaying the overall failure of column elements. Notably, substantial yielding in the hybrid-strengthened specimen prior to failure prevented the premature debonding of the FRCM layers.

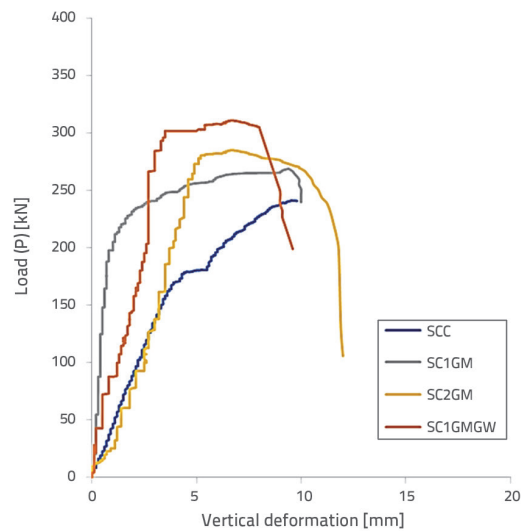


Figure 13. Load vs. deformation of :1) SCC, 2) SC1GM, 3) SC2GM, 4) SC1GMGC

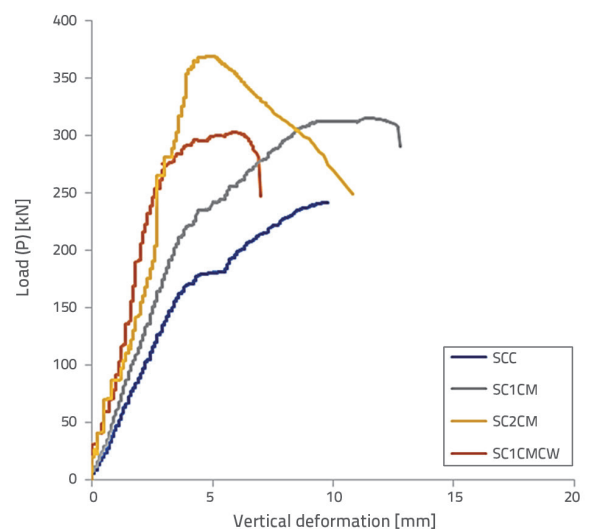


Figure 14. Load vs. deformation of: 1) SCC; 2) SC1CM; 3) SC2CM; 4) SC1CMCC

Table 7. Area under the load–deformation curve up to peak

No.	Specimen designation	Area under load deformation curve up to peak [kN/mm]
1	SCC	1574
2	SC1GM	2391
3	SC2GM	2388
4	SC1GMGW	2457
5	SC1CM	2581
6	SC2CM	2861
7	SC1CMCW	2965

Table 8. Maximum tie strain values

Specimen ID	Maximum strain at end tie [micrometre]	Maximum strain at middle tie [micrometre]
CCC	2270	765
CC1GM	962	503
CC2GM	798	443
CC1GMGW	695	325
CC1CM	896	496
CC2CM	801	333
CC1CMCW	669	305

4.3. Ductility

The ductility characteristics of the materials were measured by calculating their energy absorption. Table 7 shows the energy absorption for each specimen which was calculated using the area under the curve of the load–deformation curve. In FRCM/EB-FRP, a higher energy absorption of 20 % to 25 % compared with the FRCM-strengthened specimen was observed. This confirms that the external FRP bonding is more confined than the FRCM layer and increases the energy absorption capacity. Higher ductility resulted in higher deformation before the failure of the column.

4.4. Tie strains

The maximum local point strains at the middle and end ties of each specimen are listed in Table 8. It was observed that the contribution of the middle tie was less than that of the end tie, owing to the concentration of the reaction at the end of the column. Because of the strengthening of the column specimen, all strengthened specimens had lower strain values than the control specimen (SCC) owing to the confinement effect of the FRP. The hybrid-strengthened specimens (i.e. SC1GMGW and SC1CMCW) had lower strain values than the single/double FRCM strengthened specimens (i.e. SC1GM, SC2GM, SC1CM, and SC2CM) because of the contribution of the external FRP wrapping towards the applied load. The strains of the carbon FRP-strengthened specimens were lower than those of the glass specimens.

4.5. Failure pattern

The failure patterns of the control and strengthened specimens are shown in Figures 15 and 16, respectively. The control specimen failed due to concrete crushing, preceded by the propagation of visible cracks at the bottom of the column, i.e. reaction point. Single- or double-layer FRCM-strengthened specimens such as SC1GM, SC2GM, SC1CM, and SC2CM experienced fibre yielding followed by layer separation/slippage, and ultimately failed by core concrete crushing, as shown in Figure 15.a and 15.c and Figure 16.b and 16.c. The failure of the FRCM layer was initiated at the end of the column owing to the high concentration of stress. The hybrid-strengthened specimens SC1GMGW and SC1CMCW failed owing to tearing of the FRP wrapping and cracking of the epoxy bonds, as shown in Figures 15.d and 16.c. In the hybrid-strengthened specimen, the external FRP wrapping confined the FRCM layer and eliminated its premature delamination of the FRCM layer. After breaking the FRP wrapping, the FRCM layers underwent internal stress and the inorganic matrix started cracking, followed by concrete crushing. In SC1GMGW and SC1CMCW columns, the wrinkles were observed in the external FRP confinement. These wrinkles indicate the debonding of the FRP or cracking of the epoxy layer. All strengthened and control specimens ultimately failed by concrete crushing at the constrained end of the column. This may be due to the lower grade of the mix proportions used.

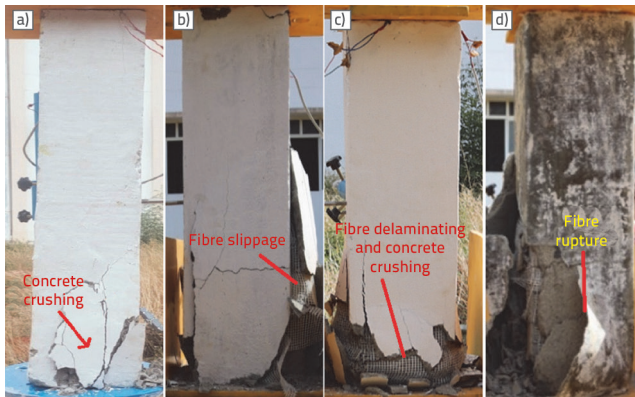


Figure 15. Mode of failure of the specimens a) SCC, b) SC1GM, c) SC2GM, and d) SC1GMGC

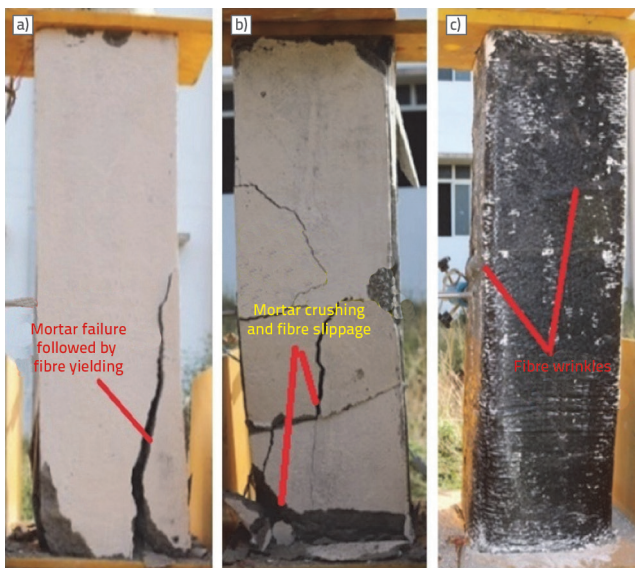


Figure 16. Mode of failure of the specimens a) SC1CM, b) SC2CM, and c) SC1CMCC

5. Conclusions

This study investigated the failure behaviour of hybrid-strengthened RC square columns using the FRCM/EB-FRP technique with both experimental and analytical methods. All columns were tested under axial compression. From the discussion, the following main inferences were made:

- The experimental investigation confirmed that the confinement of all the strengthened specimens produced a higher capacity and ductility than the unconfined specimen. The hybrid specimens exhibited a 25%–65% higher ultimate strength than the single/double-layer FRCM. The hybrid method proved to be more effective than FRCM alone.
- Carbon FRP contributed more to strengthening than glass FRP because of its higher tensile strength. In these experiments, the hybrid-strengthened specimens were strengthened with the same type of fibres used in both the FRCM and external FRP. The hybrid specimen with carbon fibres exhibited a better performance in terms of strength and stiffness than the hybrid specimen with glass fibres.
- The hybrid FRCM/EP-FRP strengthening technique showed that the number of FRCM layers can be reduced using external FRP bonding, thereby decreasing the overlay thickness of the strengthened column in the FRCM.
- The hybrid-strengthened columns using both glass and carbon types exhibited similar behaviours. The strength and stiffness of the carbon specimens were higher because of their higher tensile capacities.
- All the strengthened specimens failed by fibre rupture, followed by concrete crushing. The failure of the FRCM-strengthened specimen occurred owing to fibre slippage, and it was diminished by the confinement of the external FRP wrapping in the hybrid method. The edge effect in the square column was reduced by the corner radius.
- The proposed hybrid method exhibited better deformation characteristics than its counterparts by absorbing more energy. This confirms that the external FRP bonding confines the FRCM layer and increases the energy absorption.
- The effectiveness of hybrid FRP strengthening can be improved by providing the FRP laminates with a higher elastic modulus; thus, the axial compressive capacity can be enhanced.

REFERENCES

- [1] Saini, A., Prakash, S.S.: Analytical study on the effectiveness of hybrid FRP strengthening on behaviour of slender reinforced concrete square columns, *Structures*, 33 (2021), pp. 4218–4242
- [2] Chellapandian, M., Prakash, S.S., Sharma, A.: Experimental and finite element studies on the flexural behavior of reinforced concrete elements strengthened with hybrid FRP technique, *Composite Structures*, 208 (2019), pp. 466–478
- [3] Fossetti, M., Alotta, G., Basone, F., Macaluso, G.: Simplified analytical models for compressed concrete columns confined by FRP and FRCM system, *Materials and Structures*, 50 (2017), pp. 1–20
- [4] Mohsen, D., Alireza, M., Mohammad, S.R., Jafar, A.M.: Performance of reinforced engineered cementitious composite square columns, *GRAĐEVINAR*, 75 (2023) 1, pp. 13–21, <https://doi.org/10.14256/JCE.3503.2022>
- [5] Harba, I.S., Abdulridha, A.J.: Numerical analysis of RC columns under cyclic uniaxial and biaxial lateral load, *GRAĐEVINAR*, 73 (2021) 10, pp. 979–994, <https://doi.org/10.14256/JCE.2889.2020>
- [6] Kernou, N., Messaoudene, L., Lyacine, B.: Effects of column damage on the reliability of reinforced concrete portal frames, *GRAĐEVINAR*, 75 (2023) 1, pp. 53–63, <https://doi.org/10.14256/JCE.3588.2022>
- [7] El-Hacha, R., Mashrik, M.A.: Effect of SFRP confinement on circular and square concrete columns, *Engineering Structures*, 36 (2012), pp. 379–393
- [8] Faleschini, F., Zanini, M.A., Hofer, L., Pellegrino, C.: Experimental behavior of reinforced concrete columns confined with carbon - FRCM composites, *Construction and Building Materials*, 243 (2020), Paper 18296

- [9] Arabshahi, A., Tavakkolizadeh, M.: Predictive model for slenderness limit of circular RC columns confined with FRP wraps, *Structural Concrete*, 23 (2022) 2, pp. 849-875
- [10] Faleschini, F., Gonzalez-Libreros, J., Zanini, M.A., Hofer, L., Sneed, L., Pellegrino, C.: Repair of severely-damaged RC exterior beam-column joints with FRP and FRCM composites, *Composite Structures*, 207 (2019), pp. 352-363
- [11] Jawdhari, A., Adheem, A.H., Kadhim, M.M.: Parametric 3D finite element analysis of FRCM-confined RC columns under eccentric loading, *Engineering Structures*, 212 (2020), Paper 110504
- [12] Ebead, U., Wakjira, T.G.: Behaviour of RC beams strengthened in shear using near surface embedded FRCM, *InIOP Conference Series: Materials Science and Engineering*, 2018.
- [13] Gonzalez-Libreros, J.H., Sneed, L.H., D'Antino, T., Pellegrino, C.: Behavior of RC beams strengthened in shear with FRP and FRCM composites, *Engineering Structures*, 150 (2017), pp. 830-842
- [14] Ombres, L., Verre, S.: Numerical modeling approaches of FRCMs/SRG confined masonry columns, *Frontiers in Built Environment*, 5 (2019), pp. 143
- [15] Chellapandian, M., Prakash, S.S., Rajagopal, A.: Analytical and finite element studies on hybrid FRP strengthened RC column elements under axial and eccentric compression, *Composite Structures*, 184 (2018), pp. 234-248
- [16] Hasan, H., Pascu, R., Georgescu, D.P.: Experimental and numerical investigation of plain concrete columns strengthening by FRCM composite material, *InIOP Conference Series: Earth and Environmental Science*, 2021.
- [17] Toska, K., Faleschini, F.: FRCM-confined concrete: monotonic vs. cyclic axial loading, *Composite Structures*, (2021), pp. 268
- [18] Gonzalez-Libreros, J., Zanini, M.A., Faleschini, F., Pellegrino, C.: Confinement of low-strength concrete with fiber reinforced cementitious matrix (FRCM) composites, *Composites, Part B: Engineering*, (2019), pp. 177
- [19] Donnini, J., Spagnuolo, S., Corinaldesi, V.: A comparison between the use of FRP, FRCM and HPM for concrete confinement, *Composites, Part B: Engineering*, 169 (2019), pp. 586-594
- [20] Jiang, T., Teng, J.G.: Behavior and design of slender FRP-confined circular RC columns, *Journal of Composites for Construction*, 17 (2013) 4, pp. 443-453
- [21] Pessiki, S., Harries, K.A., Kestner, J.T., Sause, R., Ricles, J.M.: Axial behavior of reinforced concrete columns confined with FRP jackets, *Journal of composites for Construction*, 5 (2001), pp. 237-245
- [22] Toutanji, H., Han, M., Gilbert, J., Matthys, S.: Behavior of large-scale rectangular columns confined with FRP composites, *Journal of Composites for Construction*, 14 (2010), pp. 62-71
- [23] Sharma, S.S., Dave, U.V., Solanki, H.: FRP wrapping for RC columns with varying corner, *Procedia engineering*, 51 (2013), pp. 220-229
- [24] Xiao, Y., Wu, H.: Compressive behavior of concrete confined by carbon fiber composite jackets, *Journal of materials in civil engineering*, 12 (2000), pp. 139-146
- [25] Kyaure, M., Abed, F.: Finite element parametric analysis of RC columns strengthened with FRCM, *Composite Structures*, 275 (2021), Paper 114498
- [26] Abu Obaida, F., El-Maaddawy, T., El-Hassan, H.: Bond behavior of carbon fabric-reinforced matrix composites: Geopolymeric matrix versus cementitious mortar, *Buildings*, 11 (2021), Paper 207
- [27] Wei, L., Ueda, T., Matsumoto, K., Zhu, J.H.: Experimental and analytical study on the behavior of RC beams with externally bonded carbon-FRCM composites, *Composite Structures*, 273 (2021), Paper 114291
- [28] Tello, N., Alhoubi, Y., Abed, F., El Refai, A., El-Maaddawy, T.: Circular and square columns strengthened with FRCM under concentric load, *Composite Structures*, 255 (2021), Paper 113000
- [29] Colajanni, P., De Domenico, F., Recupero, A., Spinella, N.: Concrete columns confined with fibre reinforced cementitious mortars: Experimentation and modelling, *Construction and Building Materials*, 52 (2014), pp. 375-384
- [30] Colajanni, P., Fossetti, M., Macaluso, G.: Effects of confinement level, cross-section shape and corner radius on the cyclic behavior of CFRM confined concrete columns, *Construction and Building Materials*, 55 (2014), pp. 379-389
- [31] Triantafyllou, T.C., Papanicolaou, C.G., Zissimopoulos, P., Laourdekis, T.: Concrete confinement with textile-reinforced mortar jackets, *ACI Structural Journal*, 103 (2006) 1, Paper 28
- [32] Feng, R., Li, Y., Zhu, J.H., Xing, F.: Behavior of corroded circular RC columns strengthened by C-FRCM under cyclic loading, *Engineering Structures*, 226 (2021), Paper111311
- [33] Zhu, J.H., Chen, J., Feng, Y., Liu, C.B.: Compression tests of C-FRCM jacket confined hollow section RC columns, *Structures*, 31 (2021) 6, pp. 961-969
- [34] Trapko, T., Musiał, M.: Effect of PBO-FRCM reinforcement on stiffness of eccentrically compressed reinforced concrete columns, *Materials*, 13 (2020) 5, Paper 1221
- [35] Chellapandian, M., Prakash, S.S., Mahadik, V., Sharma, A.: Experimental and numerical studies on effectiveness of hybrid FRP strengthening on behavior of RC columns under high eccentric compression, *Journal of Bridge Engineering*, 24 (2019) 6, pp. 04019048
- [36] Ispir, M., Dalgic, K.D., Ilki, A.: Hybrid confinement of concrete through use of low and high rupture strain FRP, *Composites, Part B: Engineering*, 153 (2018), pp. 243-255
- [37] Noroozieh, E., Mansouri, A.: Lateral strength and ductility of reinforced concrete columns strengthened with NSM FRP rebars and FRP jacket, *International Journal of Advanced Structural Engineering*, 11 (2019) 2, pp. 195-209
- [38] Wakjira, T.G., Ebead, U.: Hybrid NSE/EB technique for shear strengthening of reinforced concrete beams using FRCM: Experimental study, *Construction and Building Materials*, 164 (2018), pp. 164-177
- [39] Ebad, U., Wakjira, T.G.: NSE/EB-FRCM technique for strengthening of RC beams in shear, *Proceedings of the 8th Euro-American Congress on Construction Pathology, Rehabilitation Technology and Heritage Management, REHABEND, Granada, Spain, 2020.*
- [40] El-Sherif, H., Wakjira, T.G., Ebead, U.: Flexural strengthening of reinforced concrete beams using hybrid near-surface embedded/externally bonded fabric-reinforced cementitious matrix, *Construction and Building Materials*, 238 (2020). pp. 117748
- [41] Ali, D., Yigit, I., Taha, Y.A.: Experimental and numerical investigation of RC beams strengthened with CFRP composites, *GRAĐEVINAR*, 73 (2021), pp. 605-616
- [42] Sumathi, M., Greeshma, S.: Experimental investigation of exterior reinforced concrete beam - column joints strengthened with hybrid FRP laminates, *GRAĐEVINAR*, 73 (2021), pp. 365-379
- [43] Hognestad, E., Hanson, N.W., McHenry, D.: Concrete stress distribution in ultimate strength design, *ACI Journal Proceedings*, 52 (1955), pp. 475-479
- [44] Hognestad, E.: A study of combined bending and axial load in RC members, *Engineering Experiment Station, University of Illinois, 1951., Bulletin 339.*
- [45] Lam, L., Teng, J.G.: Design oriented stress strain model for FRP confined concrete in rectangular columns, *Journal of Reinforced Plastics and Composites*, 22 (2003), pp. 1149-1186
- [46] Lam, L., Teng, J.G.: Design oriented stress strain model for FRP confined concrete, *Construction Building Materials*, 17 (2003), pp. 471-489
- [47] Mander, J.B., Priestley, M.J.N., Park, R.: Theoretical σ - ϵ model for confined concrete, *ASCE Journal of Structural Engineering*, 114 (1988) 8, pp. 1804-1826
- [48] Popovics, S.: Numerical approach to the complete σ - ϵ relation for concrete, *Cement and concrete composites*, 3 (1973) 5, pp. 583-599